A 4-link Model of a Human for Simulating a Forward Fall

Dariusz GRZELCZYK
Lodz University of Technology, Department of Automation, Biomechanics and Mechatronics, 1/15 Stefanowski Str., 90-924 Lodz, Poland, dariusz.grzelczyk@p.lodz.pl

Paweł BIESIACKI
Lodz University of Technology, Department of Automation, Biomechanics and Mechatronics, 1/15 Stefanowski Str., 90-924 Lodz, Poland, pawelbiesiacki@o2.pl

Jerzy MROZOWSKI
Lodz University of Technology, Department of Automation, Biomechanics and Mechatronics, 1/15 Stefanowski Str., 90-924 Lodz, Poland, jerzy.mrozowski@p.lodz.pl

Jan AWREJCEWICZ
Lodz University of Technology, Department of Automation, Biomechanics and Mechatronics, 1/15 Stefanowski Str., 90-924 Lodz, Poland, jan.awrejcewicz@p.lodz.pl

Abstract

In this paper we consider a 4-link model of a human for simulating a forward fall. The model implemented in Mathematica is constructed based on a planar mechanical system with a non-linear impact law modelling the wrist-ground contact. The segments of the human body are modelled as bodies connected by rotary elements which correspond to the human joints. Parameters and kinematic relations used in numerical analysis are obtained based on the 3D scanned model of the human body created in Inventor and experimental observation by the motion capture system. Validation of the model is conducted by means of comparing the simulation of the impact force with the experimental data obtained from the force platform. The obtained ground reaction forces can be useful for the finite element analysis of the numerical model of the human upper extremity.

Keywords: forward fall, ground reaction force, bone strength, upper extremity, distal radius

1. Introduction

A fall onto outstretched arms belongs to the one of the main reasons of the upper limb bone injuries. The resulting bone fractures are a serious both medical and social problem due to long-term sick leave, absence from work, or sometimes a complicated rehabilitation process, especially among the elderly [1, 2]. The upper limb injuries may be the result of forward falls, backward falls or side ones. However, a forward fall is the most common type of fall and more than a half of all falls among the elderly occur in the forward direction. Usually, upper extremity injuries result from a forward fall with direct impact on the fully extended upper extremities [3, 4]. Due to the weakened bone quality/density and the increased risk of falling, distal radius fractures are especially common in eldery women with osteoporosis.

The so-called Colles' fracture, which is an injury of distal radius of a forearm, is the most common type of fracture of the upper extremity resulting from a forward fall [5]. Colles' fracture is a direct result of exceeding the maximum value of force allowable for

this bone. Evaluation of this value (known as a distal radius fracture threshold) has been the research goal of numerous scientists. Distal radius fractures at a mean force equal to 1640 ± 980 N were observed by Spadaro and his co-investigators [6]. Kim and Ashton-Miller used the value equal to 2400 N as a distal radius fracture threshold in their investigations [7]. Recently, also Burkhart and his co-investigators tested real bones from cadavers and the obtained value of the distal radius fracture threshold equal approximately to 2150 N [8].

In order to understand the biomechanical factors having the greatest impact on the risk injury, different fall models have been proposed [7, 9-11]. Numerous papers have presented linear or non-linear spring-damper models for modelling of contact with the ground in various types of motion [10, 12-17]. In this paper we proposed another mathematical model of the human forward fall on outstretched arms. Mechanical, kinematical, and dynamical parameters of this model were identified using experimental investigations of a real falling process. Moreover, we investigated the influence of different human walking speed just before a trip over an obstacle and starting the falling process, which affects the ground reaction force (GRF) acting on the upper extremity.

2. Forward fall model

A scheme of a human forward fall on outstretched arms is presented schematically in Fig. 1 as a flat 4-DoFs mechanical model.

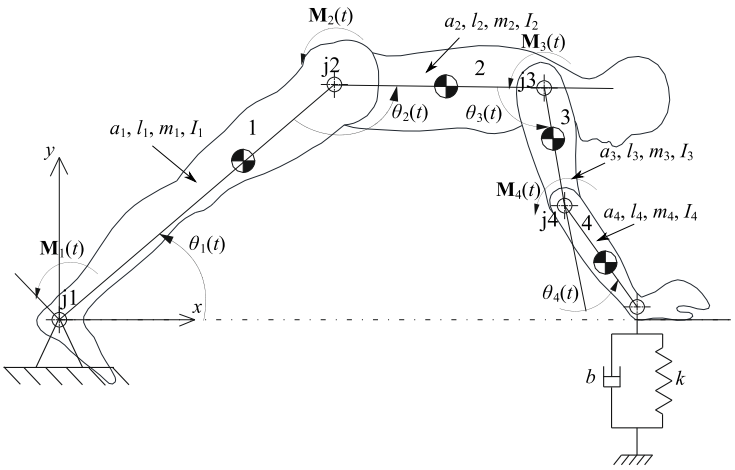

Figure 1. The proposed forward fall model with 4-DoFs

The presented model consists of four bodies (i = 1, 2, 3, 4), i.e. lower extremities, torso (with neck and head), arms and forearms, characterized by masses m_i, moments of inertia I_i about centres of the masses, the total lengths l_i of the links between the joints and the lengths a_i between the joints j1, j2, j3, j4, and centres of gravity of masses m_i, respectively. Definitions of the angles $\theta_i(t)$ are also given in Fig. 1.

Equations of motion governing the considered system were obtained using the Newton-Euler method. To do it, we took the vectors of angles $\boldsymbol{\theta}_i(t)=\left[0,0,\theta_i(t)\right]^T$ and the following vectors:

$$\mathbf{r}_1(t)=\left[x_1(t),y_1(t),0\right]^T=\left[a_1\cos\theta_1(t),a_1\sin\theta_1(t),0\right]^T, \tag{1}$$

$$\mathbf{r}_2(t)=\left[x_2(t),y_2(t),0\right]^T=\left[l_1\cos\theta_1(t)+a_2\cos\alpha(t),l_1\sin\theta_1(t)-a_2\sin\alpha(t),0\right]^T, \tag{2}$$

$$\mathbf{r}_3(t)=\left[x_3(t),y_3(t),0\right]^T=\begin{bmatrix}l_1\cos\theta_1(t)+l_2\cos\alpha(t)+a_3\cos\beta(t)\\ l_1\sin\theta_1(t)-l_2\sin\alpha(t)-a_3\sin\beta(t)\\ 0\end{bmatrix}, \tag{3}$$

$$\mathbf{r}_4(t)=\left[x_4(t),y_4(t),0\right]^T=\begin{bmatrix}l_1\cos\theta_1(t)+l_2\cos\alpha(t)+l_3\cos\beta(t)+a_4\cos\gamma(t)\\ l_1\sin\theta_1(t)-l_2\sin\alpha(t)-l_3\sin\beta(t)-a_4\sin\gamma(t)\\ 0\end{bmatrix}, \tag{4}$$

$$\mathbf{l}_1(t)=\left[l_1\cos\theta_1(t),l_1\sin\theta_1(t),0\right]^T, \tag{5}$$

$$\mathbf{l}_2(t)=\left[l_1\cos\theta_1(t)+l_2\cos\alpha(t),l_1\sin\theta_1(t)-l_2\sin\alpha(t),0\right]^T, \tag{6}$$

$$\mathbf{l}_3(t)=\begin{bmatrix}l_1\cos\theta_1(t)+l_2\cos\alpha(t)+l_3\cos\beta(t)\\ l_1\sin\theta_1(t)-l_2\sin\alpha(t)-l_3\sin\beta(t)\\ 0\end{bmatrix}, \tag{7}$$

$$\mathbf{l}_4(t)=\begin{bmatrix}l_1\cos\theta_1(t)+l_2\cos\alpha(t)+l_3\cos\beta(t)+l_4\cos\gamma(t)\\ l_1\sin\theta_1(t)-l_2\sin\alpha(t)-l_3\sin\beta(t)-l_4\sin\gamma(t)\\ 0\end{bmatrix}, \tag{8}$$

where $\alpha(t)=\pi-\theta_1(t)-\theta_2(t)$, $\beta(t)=\pi+\alpha(t)-\theta_3(t)$ and $\gamma(t)=\beta(t)-\theta_4(t)$. Forces $\mathbf{Q}_1=\left[0,-m_1g,0\right]^T$, $\mathbf{Q}_2=\left[0,-m_2g,0\right]^T$, $\mathbf{Q}_3=\left[0,-m_3g,0\right]^T$, and $\mathbf{Q}_4=\left[0,-m_4g,0\right]^T$ are the gravity forces acting on the centre of gravity of bodies 1, 2, 3, and 4, respectively, where $g=9.81\ \mathrm{m/s^2}$ denotes gravity coefficient. The force $\mathbf{R}(t)=\left[R_x(t),R_y(t),0\right]^T$ is the reaction force in the joint j1. The unknown joint forces (resulting from presentation of the considered system as a free body diagram) are denoted as $\mathbf{P}_1(t)=\left[P_{1x}(t),P_{1y}(t),0\right]^T$, $\mathbf{P}_2(t)=\left[P_{2x}(t),P_{2y}(t),0\right]^T$, and $\mathbf{P}_3(t)=\left[P_{3x}(t),P_{3y}(t),0\right]^T$, respectively. Finally, the force $\mathbf{F}(t)=\left[F_x(t),F_y(t),0\right]^T$ is the ground reaction force acting on the body 4 at the moment of impact to the ground.

Let us assume that $\mathbf{M}_1(t)=\left[0,0,0\right]^T$, $\mathbf{M}_2(t)=\left[0,0,M_2(t)\right]^T$, $\mathbf{M}_3(t)=\left[0,0,M_3(t)\right]^T$, and $\mathbf{M}_4(t)=\left[0,0,M_4(t)\right]^T$ denote the torques generated in joints j1, j2, j3, and j4, respectively. Then, the analysed system can be described by the equations of motion in the following vector form:

$$m_1\ddot{\mathbf{r}}_1(t)=\mathbf{R}(t)+\mathbf{Q}_1+\mathbf{P}_1(t), \tag{9}$$

$$\begin{aligned} &I_1\ddot{\boldsymbol{\theta}}_1(t)=\mathbf{M}_1(t)-\mathbf{M}_2(t)+\boldsymbol{\tau}_{\mathbf{R}}(t)+\boldsymbol{\tau}_{\mathbf{P}12}(t)= \\ &=\mathbf{M}_1(t)-\mathbf{M}_2(t)-\mathbf{r}_1(t)\times\mathbf{R}(t)+\left[\mathbf{l}_1(t)-\mathbf{r}_1(t)\right]\times\mathbf{P}_1(t), \end{aligned} \tag{10}$$

$$m_2\ddot{\mathbf{r}}_2(t)=-\mathbf{P}_1(t)+\mathbf{Q}_2+\mathbf{P}_2(t), \tag{11}$$

$$\begin{aligned} &I_2\ddot{\boldsymbol{\theta}}_2(t)=\mathbf{M}_2(t)-\mathbf{M}_3(t)+\boldsymbol{\tau}_{\mathbf{P}21}(t)+\boldsymbol{\tau}_{\mathbf{P}23}(t)= \\ &=\mathbf{M}_2(t)-\mathbf{M}_3(t)+\left[\mathbf{l}_1(t)-\mathbf{r}_2(t)\right]\times\left[-\mathbf{P}_1(t)\right]+\left[\mathbf{l}_2(t)-\mathbf{r}_2(t)\right]\times\mathbf{P}_2(t), \end{aligned} \tag{12}$$

$$m_3\ddot{\mathbf{r}}_3(t)=-\mathbf{P}_2(t)+\mathbf{Q}_3+\mathbf{P}_3(t), \tag{13}$$

$$\begin{aligned} &I_3\ddot{\boldsymbol{\theta}}_3(t)=\mathbf{M}_3(t)-\mathbf{M}_4(t)+\boldsymbol{\tau}_{\mathbf{P}32}(t)+\boldsymbol{\tau}_{\mathbf{P}34}(t)= \\ &=\mathbf{M}_3(t)-\mathbf{M}_4(t)+\left[\mathbf{l}_2(t)-\mathbf{r}_3(t)\right]\times\left[-\mathbf{P}_2(t)\right]+\left[\mathbf{l}_3(t)-\mathbf{r}_3(t)\right]\times\mathbf{P}_3(t), \end{aligned} \tag{14}$$

$$m_4\ddot{\mathbf{r}}_4(t)=-\mathbf{P}_3(t)+\mathbf{Q}_4+\mathbf{F}(t), \tag{15}$$

$$\begin{aligned} &I_4\ddot{\boldsymbol{\theta}}_4(t)=\mathbf{M}_4(t)+\boldsymbol{\tau}_{\mathbf{P}43}(t)+\boldsymbol{\tau}_{\mathbf{F}}(t)= \\ &=\mathbf{M}_4(t)+\left[\mathbf{l}_3(t)-\mathbf{r}_4(t)\right]\times\left[-\mathbf{P}_3(t)\right]+\left[\mathbf{l}_4(t)-\mathbf{r}_4(t)\right]\times\mathbf{F}(t), \end{aligned} \tag{16}$$

where $\boldsymbol{\tau}_{\mathbf{R}}(t)$, $\boldsymbol{\tau}_{\mathbf{P}12}(t)$, $\boldsymbol{\tau}_{\mathbf{P}21}(t)$, $\boldsymbol{\tau}_{\mathbf{P}23}(t)$, $\boldsymbol{\tau}_{\mathbf{P}32}(t)$, $\boldsymbol{\tau}_{\mathbf{P}34}(t)$, $\boldsymbol{\tau}_{\mathbf{P}43}(t)$, $\boldsymbol{\tau}_{\mathbf{F}}(t)$ are torques generated by forces $\mathbf{R}(t)$, $\mathbf{P}_1(t)$, $\mathbf{P}_2(t)$, $\mathbf{P}_3(t)$ and $\mathbf{F}(t)$.

At the moment of tripping over an obstacle, the faller instinctively bends in the hip joint and pulls their upper extremities (arms and forearms) to the front to arrest and/or absorb the fall. Taking into account the abovementioned kinematic excitations (described by functions $\theta_2(t)$, $\theta_3(t)$, and $\theta_4(t)$, respectively), the considered system can be reduced to the single DoF model described by the following equation of motion

$$\begin{aligned} &I_1\ddot{\boldsymbol{\theta}}_1(t)+I_2\ddot{\boldsymbol{\theta}}_2(t)+I_3\ddot{\boldsymbol{\theta}}_3(t)+I_4\ddot{\boldsymbol{\theta}}_4(t)=-\mathbf{r}_1(t)\times\mathbf{R}(t)+\left[\mathbf{l}_1(t)-\mathbf{r}_1(t)\right]\times\mathbf{P}_1(t)+ \\ &+\left[\mathbf{l}_1(t)-\mathbf{r}_2(t)\right]\times\left[-\mathbf{P}_1(t)\right]+\left[\mathbf{l}_2(t)-\mathbf{r}_2(t)\right]\times\mathbf{P}_2(t)+ \\ &+\left[\mathbf{l}_2(t)-\mathbf{r}_3(t)\right]\times\left[-\mathbf{P}_2(t)\right]+\left[\mathbf{l}_3(t)-\mathbf{r}_3(t)\right]\times\mathbf{P}_3(t)+ \\ &+\left[\mathbf{l}_3(t)-\mathbf{r}_4(t)\right]\times\left[-\mathbf{P}_3(t)\right]+\left[\mathbf{l}_4(t)-\mathbf{r}_4(t)\right]\times\mathbf{F}(t) \end{aligned} \tag{17}$$

with scalar function $\theta_1(t)$ as a solution of this equation.

To predict the vertical component of the ground reaction force, we used a non-linear model of impact at the wrist-ground interface in the form [10, 16, 17]

$$F_y(t) = k\left|y(t)\right|^3 (1 - b\dot{y}(t)) \cdot J(-y(t)), \tag{18}$$

where k and b denote ground stiffness and damping coefficient in the vertical direction, respectively, $y(t) = l_1 \sin\theta_1(t) - l_2 \sin\alpha(t) - l_3 \sin\beta(t) - l_4 \sin\gamma(t)$, while the function $J(-y(t))$ has the form

$$J(-y(t)) = \begin{cases} 1 & \text{for} \quad y(t) < 0, \\ 0 & \text{for} \quad y(t) \geq 0. \end{cases} \tag{19}$$

At the beginning of the trip, the person is usually in a standing position, and therefore we took initial angular position $\theta_1(0) = \pi/2$ (see Fig. 1). Initial angular velocity was estimated on the basis of the transverse human speed v_0 during walking just before the moment of trip according to the formula

$$I\frac{\Delta\dot{\theta}_1(t)}{\Delta t} = rF \Rightarrow \Delta\dot{\theta}_1(t) = -\frac{(m_1 + m_2 + m_3 + m_4)v_0 r}{I} = \dot{\theta}_1(0), \tag{20}$$

adopted from reference [17], where $F\Delta t$ is a force impulse causing rotation of the human body around the rotation axis placed in feet (ankles), I is the moment of inertia of the human body around the pivot axis, whereas r is the distance between the human gravity centre and the pivot axis with upper extremities adjusted along the body.

To determine the appropriate lengths, masses, and moments of inertia of the faller's body, we used the full 3D scanned human body model (see Fig. 2). Even though a human body is not a homogenous structure, we assumed the average density of the human body $\rho = 1050$ kg/m^3 to calculate these values.

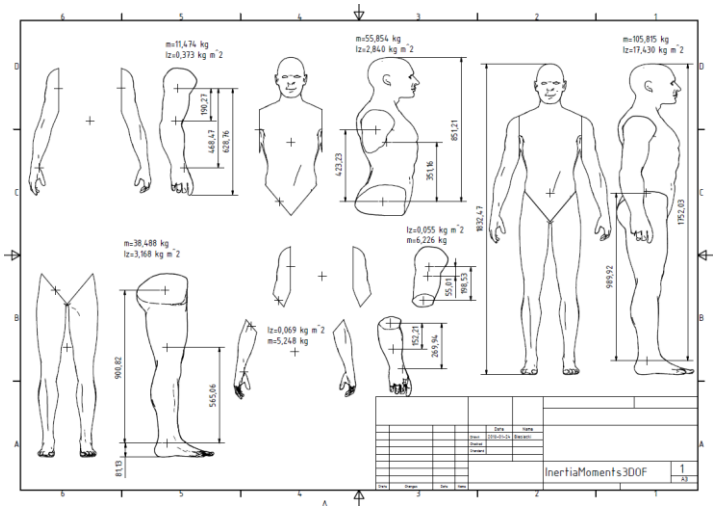

Figure 2. 3D scanned human body model analysed in Inventor

3. Experimental investigations

In our experimental investigations, kinematic of the faller from the moment of tripping over an obstacle to hitting wrists to the force platform were observed using the Optitrack system. Figure 3 presents the pictures of the faller's body configurations obtained at different times of the forward falling process. Time histories of angles $\theta_2(t)$, $\theta_3(t)$, and $\theta_4(t)$ obtained from the experiment are depicted in Fig. 4.

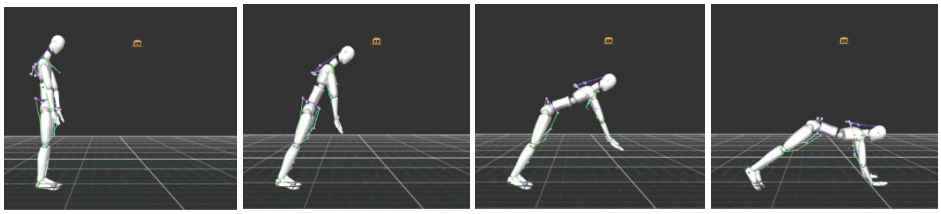

Figure 3. Pictures of the faller's body configurations at different times of the falling process, obtained experimentally

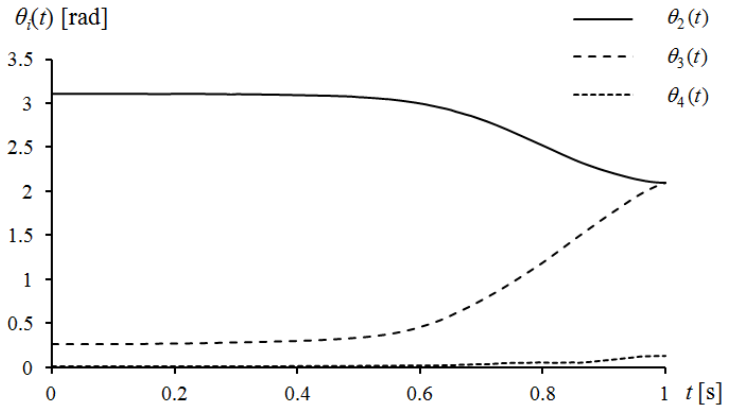

Figure 4. Time histories of angles $\theta_2(t)$, $\theta_3(t)$, and $\theta_4(t)$ obtained from the experiment

Figure 5 shows the real time histories of the impact force acting on the single hand of the faller, registered during the experiment using the force platform. As can be seen, the impact force increases from zero to a maximum value of about 1500 N during the time about 0.05 s. Next, the force changes periodically and decreases to about 400 N during the time interval 1.0 - 1.2 s.

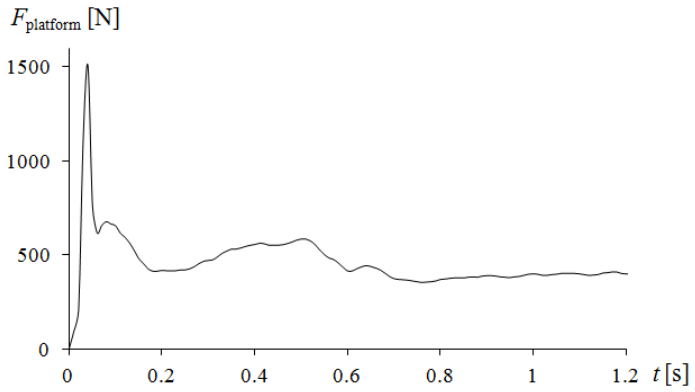

Figure 5. Time history of GRF obtained experimentally by using a force platform

To carry out numerical simulations of the proposed fall model, we adopted parameters $k = 3500$ kN/m^3 and $b = 6.0$ s/m based on the paper [10]. Is should be noted that the human body is a complicated biomechanical system, which contains numerous different muscles that absorb the impact force during a fall. Therefore, in case of a real fall to the ground, a part of the impact energy is absorbed by the abovementioned muscles, which are not considered in this fall model. By comparing the real ground reaction force obtained from the dynamometric platform and the impact force generated by the proposed fall model, we calculated what a part of the impact energy (impact force) is transferred to the upper extremities, and what a part is dissipated in other parts of the human body. By extrapolating the proposed model, it is possible to evaluate the real value of the impact force acting on the faller during impact to the ground for different values of the faller walking speed v_0 just before tripping over an obstacle.

4. Numerical simulations

The proposed forward fall model was implemented and visualised in Mathematica software. Figure 6 shows animation snapshots of the faller's body, plotted at different times of the fall from a standing position. The presented frames of the animation correspond to the fall tested experimentally and observed using the Optitrack system.

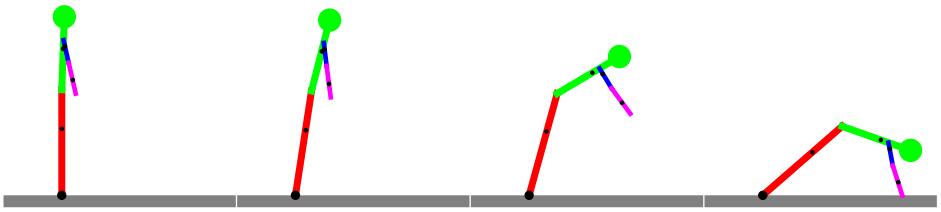

Figure 6. Snapshots of the faller's body plotted at different stages of the fall

The detailed experimental observations and experiences with falls demonstrate that with an increase in the walking speed v_0, the faller instinctively bends the body around the hip joint faster and pulls their arms (forearms) in the forward direction. As a result, the duration of the fall is shorter. Therefore, in our further numerical analysis, we used different time histories of the angles $\theta_2(t)$, $\theta_3(t)$, and $\theta_4(t)$ with different duration of the fall, depending on the speed v_0 of the human walking just before the trip.

Figure 7 shows maximum values of GRF as a function of the velocity v_0 and values of GRFs which correspond to the distal radius fracture thresholds adopted from other references [6-8]. The maximum value of GRF increases with the increasing speed v_0. For the lowest presented value of v_0 (equal to 0.5 m/s), the estimated maximum value of GRF is 1611 N. For the largest value of v_0 (equal to 3.0 m/s), the maximum value of GRF is 2629 N. As a result, for small values of v_0, the maximum value of GRF is less than the presented distal radius fracture thresholds. For large value of v_0, the maximum GRF exceeds all the presented distal radius fracture thresholds. Moreover, for a large walking speed of human gait before the falling process, the value of the distal radius fracture threshold is usually exceeded, eventually leading to injuries and/or fractures of the upper extremities. Concluding, for instance, the presented results and further extrapolation of the proposed fall model can be suitable for the finite element analysis of the numerical model of the human upper extremity as a load condition.

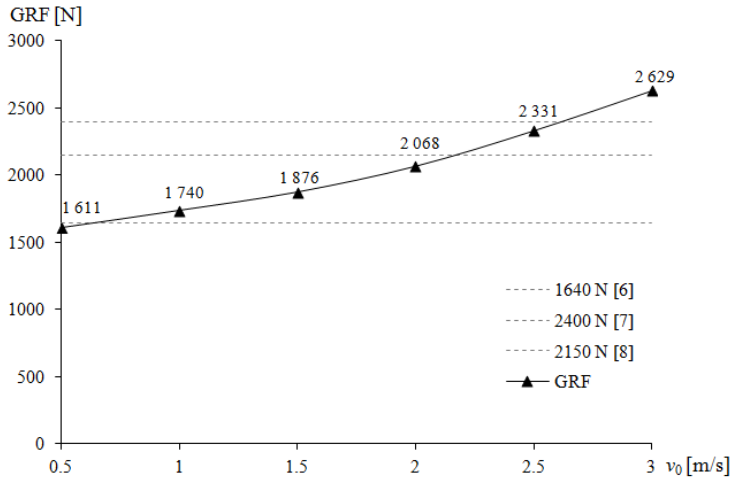

Figure 7. Distal radius fracture thresholds [6-8] and maximum values of GRF as a function of velocity v_0

5. Conclusions

The paper presents a 4-link mechanical model implemented in Mathematica, useful for simulation of the human forward fall on outstretched arms. The considered model is an extension of the forward fall models presented in references [17, 18]. The model enables to estimate the vertical ground reaction force acting on the hands during the falling process. The appropriate segments of the human body are modelled as four rigid bodies connected by three rotary joints, which correspond to the human hip, shoulder, and elbow joints. To estimate parameters of the faller body, we used three-dimensional scanned human body model created and segmented in Inventor. Kinematics of the falling process was observed by the Optitrack system, while the real ground reaction force during the impact to the ground was registered by the force platform. The proposed fall model allows to estimate the value of the vertical ground reaction force acting on the hands of the faller during the impact to the ground for different speed just before tripping over an obstacle.

It should be noted that the developed model has also some limitations. The movement of the shoulder grid with respect of the torso and stiffness/damping properties of the shoulder, hip and/or elbow joints have not been considered in the presented analysis. Also, only the vertical component of the ground reaction force has been considered, whereas the horizontal component has been neglected. Nevertheless, the presented forward fall model enables to obtain the results, which can be used, for instance, for finite element analysis of the human upper extremity.

Ethical approval

This article does not contain any studies performed on animals. The presented experimental studies have been performed on one of the authors of this paper (Paweł Biesiacki) without any other human participants.

Acknowledgments

The work has been supported by the National Science Centre of Poland under the grant OPUS 9 no. 2015/17/B/ST8/01700 for years 2016-2018.

References

1. M. J. H. Heijnen, S. Rietdyk, *Falls in young adults: Perceived causes and environmental factors assessed with a daily online survey*, Hum. Movement Sci., **46** (2016) 86 – 95.
2. S. N. Robinovitch, F. Feldman, Y. Yang, R. Schonnop, P. M. Leung, T. Sarraf, et al, *Video capture of the circumstances of falls in elderly people residing in long-term care: an observational study*, Lancet, **381** (2013) 47 – 54.
3. M. C. Nevitt, S. R. Cummings, *Type of fall and risk of hip and wrist fractures: the study of osteoporotic fractures*, J. Am. Geriatr. Soc., **41** (1993) 1226 – 1234.
4. M. Palvanen, P. Kannus, J. Parkkari, T. Pitkajarvi, M. Pasanen, I. Vuori, M. Jarvinen, *The injury mechanisms of osteoporotic upper extremity fractures among*

older adults: a controlled study of 287 consecutive patients and their 108 controls, Osteoporosis Int., **11** (2000) 822 – 831.
5. O. Johnell, J. A. Kannis, *An estimate of the worldwide prevalence and disability associated with osteoporotic fractures*, Osteoporosis Int., **17** (2006) 1726 – 1733.
6. J. A. Spadaro, F. W. Werner, R. A. Brenner, M. D. Fortino, L. A. Fay, W. T. Edwards, *Cortical and trabecular bone contribute strength to the osteopenic distal radius*, J. Orthop. Res., **12** (1994) 211 – 218.
7. K.-J. Kim, J. A. Ashton-Miller, *Segmental dynamics of forward fall arrests: A system identification approach*, Clin. Biomech., **24** (2009) 348 – 354.
8. T. A. Burkhart, D. M. Andrews, C. E. Dunning, *Multivariate injury risk criteria and injury probability scores for fractures to the distal radius*, J. Biomech., **46** (2013) 973 – 978.
9. J. Chiu, S. N. Robinovitch, *Prediction of upper extremity impact forces during falls on the outstretched hand*, J. Biomech., **31** (1998) 1169 – 1176.
10. K. M. DeGoede, J. A. Ashton-Miller, *Biomechanical simulations of forward fall arrests: effects of upper extremity arrest strategy, gender and aging-related declines in muscle strength*, J. Biomech., **36** (2003) 413 – 420.
11. S. Lehner, T. Geyer, F. I. Michel, K. U. Schmitt, V. Senner, *Wrist injuries in snowboarding – Simulations of a worst case scenario of snowboard falls*, Procedia Engineer., **72**, (2014) 255 – 260.
12. M. Silva, R. Barbosa, T. Castro, *Multi-legged walking robot modelling in MATLAB/Simmechanics^{TM} and its simulation*, Proceedings of the 2013 8th EUROSIM Congress on Modelling and Simulation, EUROSIM 2013, 10-13 September 2013, Cardiff, Wales, 226 – 231.
13. G. T. Yamaguchi, *Dynamic modelling of musculoskeletal motion*, Springer-Science+Business Media, B.V., 2001.
14. F. C. Anderson, M. G. Pandy, *Dynamic optimization of human walking*, J. Biomech. Eng., **123** (2001) 381 – 390.
15. R. R. Neptune, I. C. Wright, A. J. van den Bogert, *A method for numerical simulation of single limb ground contact events: application to heel-toe running*, Comput. Method Biomec., **3** (2000) 321 – 334.
16. K. G. M. Gerritsen, A. J. van den Bogert, B. M. Nigg, *Direct dynamics simulation of the impact phase in heel-toe running*, J. Biomech., **28** (1995) 661 – 668.
17. D. Grzelczyk, P. Biesiacki, J. Mrozowski, J. Awrejcewicz,, *Dynamic simulation of a novel "broomstick" human forward fall model and finite element analysis of the radius under the impact force during fall*, J. Theor. Appl. Mech., **56** (2018) 239 – 253.
18. P. Biesiacki, J. Mrozowski, D. Grzelczyk, J. Awrejcewicz, *Modelling of forward fall on outstretched hands as a system with ground contact*, DYNAMICAL SYSTEMS: MODELLING Book Series: Springer Proceedings in Mathematics & Statistics, **181** (2016) 61 – 72.